



Journal of Mining and Earth Sciences

Website: <https://jmes.humg.edu.vn>

Determination of density value in the Nong Son - Da Nang by Petrov's 3D gravity inversion

Hong Thi Phan^{1,*}, Phuong Minh Do², Vladimirovich Aleksey Petrov³



¹Hanoi University of Mining and Geology, Hanoi, Vietnam

²Geophysical Division, Vietnam Geological and Minerals Department, Hanoi, Vietnam

³University of Geology and Exploration named Sergo Ordzhonikidze, Moscow, Russia

ARTICLE INFO

Article history:

Received 24th Nov. 2025

Revised 17th Feb. 2026

Accepted 14th Mar. 2026

Keywords:

COSCAD 3D,

Density.

Gravity field,

Nong Son - Da Nang,

Petrov's 3D inversion,

ABSTRACT

The paper presents the results of Petrov's 3D inversion applied to gravity data to determine the continuous distribution of rock density from the surface down to a depth of $Z = 7250$ m in the Nong Son - Da Nang area, supporting the delineation of potential zones associated with ore-forming processes. The inversion method was performed continuously on the residual gravity field using a two-dimensional "live-window" energy filter, with window sizes varying from 600-8600 m. The reliability of the inversion results strongly depends on the accurate determination of residual gravity anomalies. Therefore, in this study, we apply a statistical-probabilistic approach to identify adaptive filter-window geometries that are consistent with the regional anomaly trend, thereby enhancing the accuracy of residual gravity anomaly separation. The results show that, at the southwestern ore-point locations, the subsurface rock density is heterogeneous, forming blocks with positive residual-density values ranging from $0.1 \div 0.35$ g/cm³, corresponding to residual gravity anomalies of $1 \div 3.5$ mGal. The residual density anomalies within local block structures at the ore-point sites extend to depths of approximately 4000 m. The density increases from about 2.25 g/cm³ at the surface to 3.05 g/cm³ at a depth of 7250m. In the ore-bearing zones, the density varies from 2.8 g/cm³ near the surface to 3.0 g/cm³ at depths of around 4000 m, forming a continuous band extending upward from depth toward near-surface levels. The interpretation results indicate potential mineralized zones associated with the upward migration and near-surface accumulation of magma-derived materials.

Copyright © 2026 Hanoi University of Mining and Geology. All rights reserved.

*Corresponding author

E - mail: phanthihong@humg.edu.vn

DOI: 10.46326/JMES.2026.67(2).04

1. Introduction

The Nong Son - Da Nang area, located within the Kon Tum massif in central Vietnam, represents the only exposed high-grade metamorphic basement along the eastern margin of the Indochina Terrane. This region comprises a complex assemblage of magmatic, sedimentary, high-grade metamorphic, and reworked metamorphic rocks. According to comprehensive syntheses by Nguyen (2000a, 2014) and Hai et al. (2014), the area hosts a diverse range of mineral resources, among which gold mineralization is particularly noteworthy (Figure 1). Numerous ore deposits and mineral occurrences have been identified, investigated, and evaluated, several of which are currently being exploited. The physical

characteristics of these deposits can be interpreted through residual density the difference between the density of ore bodies and that of the surrounding rocks, which are reflected in the Bouguer gravity anomaly field of the study area (Figure 2). Previous geophysical investigations in this region have primarily focused on delineating the depths of major crustal interfaces such as the sedimentary, Conrad, and Moho basements. However, studies addressing density variations between ore bodies and surrounding rocks remain limited, largely due to the absence of an optimized approach suitable for the complex geological conditions of the region (Nguyen, 2000a; Nguyen, 2014; Nguyen, 2000b).

In this study, we apply Petrov's three-dimensional gravity inversion method to estimate

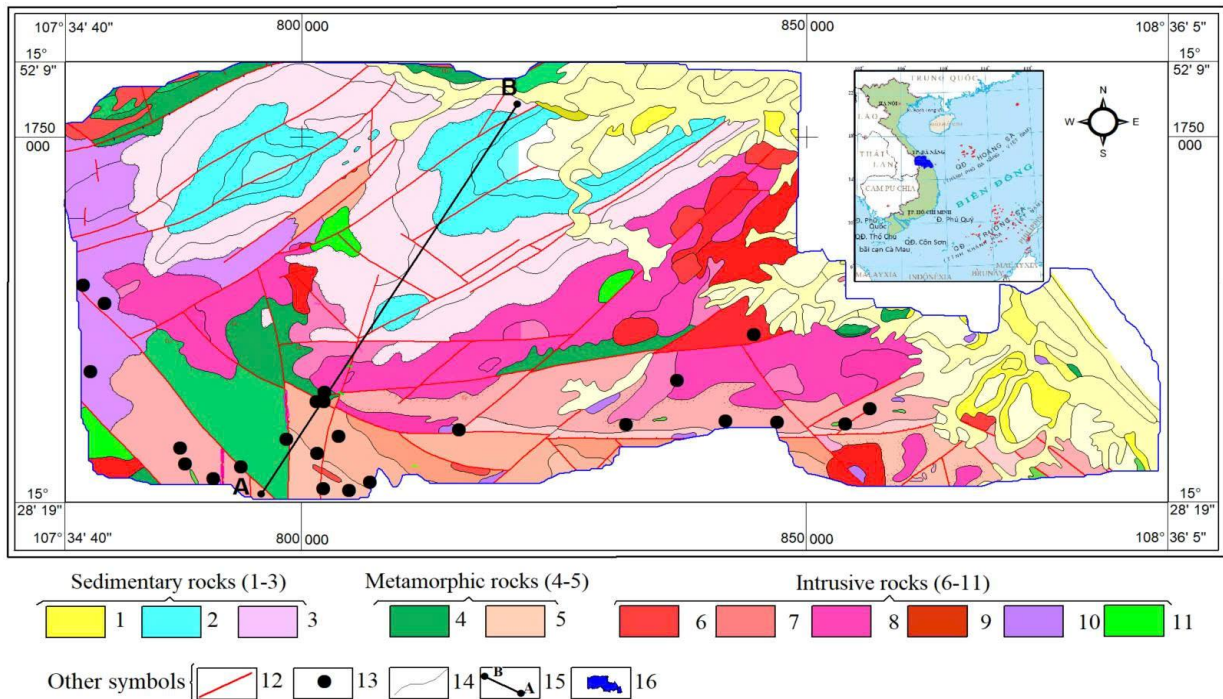


Figure 1. Location of the study area and simplified geological surface structural map of the Nong Son-Da Nang area (Nguyen and Tran, 1983; Nguyen, 1995). Sedimentary rocks (1-3): 1- Quaternary sediments and basalt; 2- Jurassic sedimentary rocks, including: Ban Co formation, Khe Ren formation, Huu Canh formation; 3- Triassic sedimentary rocks, including: Song Bung formation, Nong Son formation. Metamorphosed sedimentary rocks (4-5): 4- Cambrian - Ordovician sedimentary rocks: A Vuong formation; 5- Proterozoic metamorphosed sedimentary rocks: Kham Duc - Nui Vu formation. Intrusive Igneous rocks (6-11): 6- Cretaceous - Paleogene intrusive rocks, including: Deo Ca complex, Ba Na complex; 7- Devonian - Triassic intrusive rocks, including: Tra Bong complex, Dai Loc complex, Hai Van complex; 8- Paleozoic intrusive rocks: Ben Giang - Que Son complex; 9- Proterozoic intrusive rocks: Chu Lai complex; 10- Ultramafic rocks: Hiep Duc complex; 11- Mafic rocks: Ta Vi complex, Nui Ngoc complex, Cha Val complex. Other Features (12 - 16): 12- Faults; 13- Mineral occurrences; 14- Geological boundaries; 15- Geological - Geophysical cross section (Line A-B); 16- Boundary of the study area.

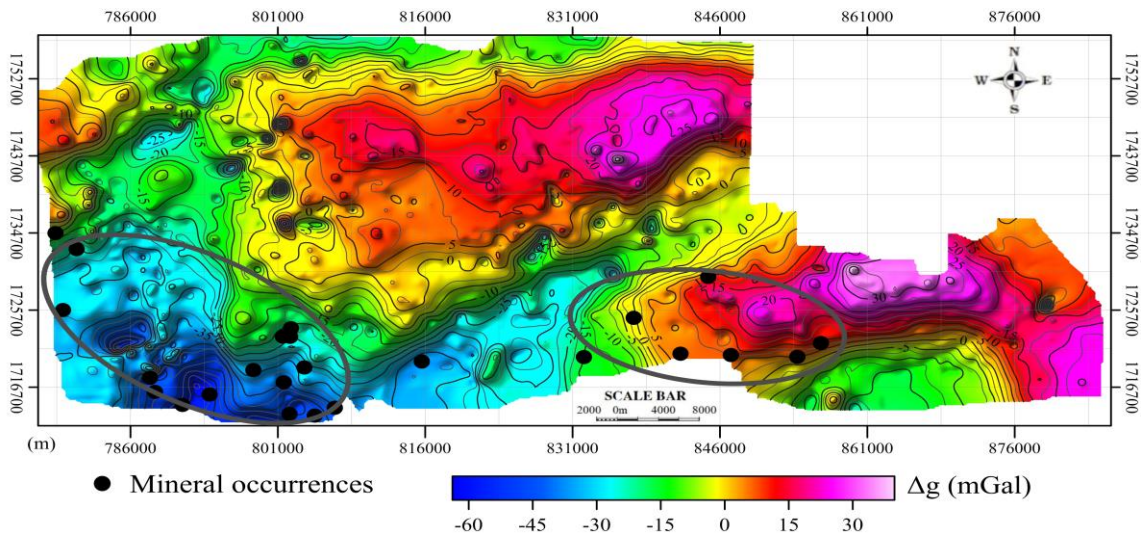


Figure 2. The full Bouguer gravitational anomaly field of the Nong Son - Da Nang, where the value varies from $-65 \div 40$ mGal.

the density of subsurface rocks. The method is based on an algorithm that integrates statistical probabilistic and spectral correlation approximations with two-dimensional “live-window” energy filter (Nikitin and Petrov, 2007; Petrov et al., 2010; Petrov et al., 2011; Petrov and Yudin, 2008), enabling a quantitative determination of the spatial characteristics of gravity anomalies, including source position, depth, and true density.

2. Data used and research methodology

2.1. Data used

The data used in this paper is the ground measured gravitational anomaly data of full Bouguer correction at the scale of 1:100.000 and the accuracy of $0.1 \div 0.25$ mGal (Nguyen, 2000a; Nguyen, 2014; Nguyen, 2000; Nguyen, 2020b). Bouguer correction density was selected as 2.67g/cm^3 and Picivanco’s method was used to correct the terrain (Blakely, 1996) and shows on Figure 2.

As shown in Figure 2, the Bouguer gravity anomaly values within the study area range from $-65 \div 40$ mGal, exhibiting a dominant northeast-southwest trend. A distinct negative anomaly belt extends along this orientation, with amplitudes between $-20 \div -5$ mGal. This belt separates two positive anomaly zones located in the northwest and southeast, where amplitudes range from $5 \div 40$ mGal. The southwestern and southern

portions of the study area are characterized by another negative anomaly belt, with amplitudes varying from $-65 \div -15$ mGal. In addition, several small-scale local anomalies, ranging from $-10 \div 10$ mGal, are observed predominantly in the northwestern and southern sectors of the area.

2.2. Research methodology

The residual density value was determined by Petrov’s 3D inversion of the residual gravity anomaly, in which the residual gravity anomaly is determined by the difference in the filter window sizes two-dimensional “live-window” energy filter is used in this study (Nikitin and Petrov, 2008; Petrov et al., 2010; Yudin, 2011; Phan et al., 2020; Phan et al., 2021; Phan, 2022; <http://www.coscad3d.ru>). The filter was built according to the changes in the spectral correlation properties of the gravity anomaly field and the noise in the studied area. The interpretation procedure used to determine the residual density value is summarised as follows:

Step 1: Two-dimensional filtering in the window of a «living» form is performed sequentially with base window dimensions 3×3 points, 5×5 points, 7×7 points, ..., $m \times n$ points, where $m \leq M/2$, $n \leq N/2$ (M , N is the maximum number of grid points of the studied area along the x and y axes). At that time the correlation radius of the two-dimensional autocorrelation function (1) is calculated in turn for each window size to determine the filter window shape.

$$R(m, n) = \frac{1}{M - |m|} \frac{1}{N - |n|} \sum_{j=1}^{N-|n|} \sum_{i=1}^{M-|m|} (f_{ij} - \bar{f})(f_{i+m, j+n} - \bar{f}) \quad (1)$$

Where: f_{ij} is field value on the j -profile at the i -point; \bar{f} is the average field over the entire survey area; M, N are consecutive total number of observation profiles along axis Ox and observation points along the Oy axis; m, n are consecutive value of the interval along axis Ox ($m = 0; \pm\Delta x; \pm 2\Delta x; \dots$) and along axis Oy ($n = 0; \pm\Delta y; \pm 2\Delta y; \dots$) represents the distance between the field values f_{ij} and $f_{i+m, j+n}$.

The filter window position is moved one grid point from left to right and from top to bottom (starting from the upper left corner and ending at the bottom right corner) over the entire survey area. To cover the field information in the leftmost and rightmost regions of the area, the filter window size is performed with the rule of decreasing window size ($k-1$) points to the last point on the profile (Petrov, 1997) (Figure 3).

According to the correlation property, the filter window shape is continuously changed to adapt to the changes of the field (Figure 4). The larger the window size, the smaller the proportion

of high-frequency local heterogeneous objects at the output of the low-pass filter.

Step 2: Calculate the residual gravity anomaly. The residual gravity anomaly is determined by the difference between the gravity anomaly of two filters with successively varying window sizes. For example, with the gravity anomalies of the filters having dimensions of 3×3 points filter being $\Delta g_{(3 \times 3) \text{ points}}$, 5×5 points filter being $\Delta g_{(5 \times 5) \text{ points}}$ and 7×7 points filter being $\Delta g_{(7 \times 7) \text{ points}}$, the residual gravity anomaly is determined by a bandpass filter is implemented (Figure 5). The larger the amplitude anomaly, the lower the frequency corresponding to it in the original field spectrum, and vice versa ..., each of these frequency ranges is associated with a certain depth interval.

Step 3: Estimate the depth Z of the filter gravity anomaly. According to Andreeva (Andreev, 1962), the depth Z of the filter gravity anomaly is related to the width of the filter window and it is estimated to be $Z \approx 0.6 \times \Delta x$ (Δx is the size of the filter window in units of length).

Step 4: Calculate residual density using the 3D inverse formula. The residual density at depth Z is calculated according to the following inverse formula (2) (Nikitin, 1986):

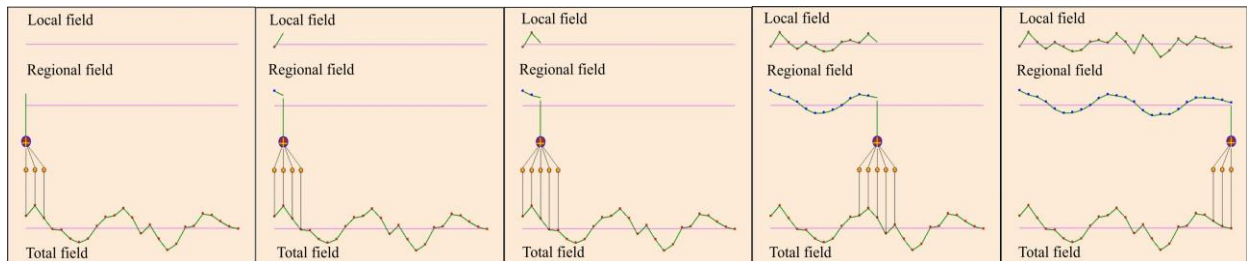


Figure 3: One-dimensional filtering in the window of a «living» form with the 5 points window sizes.

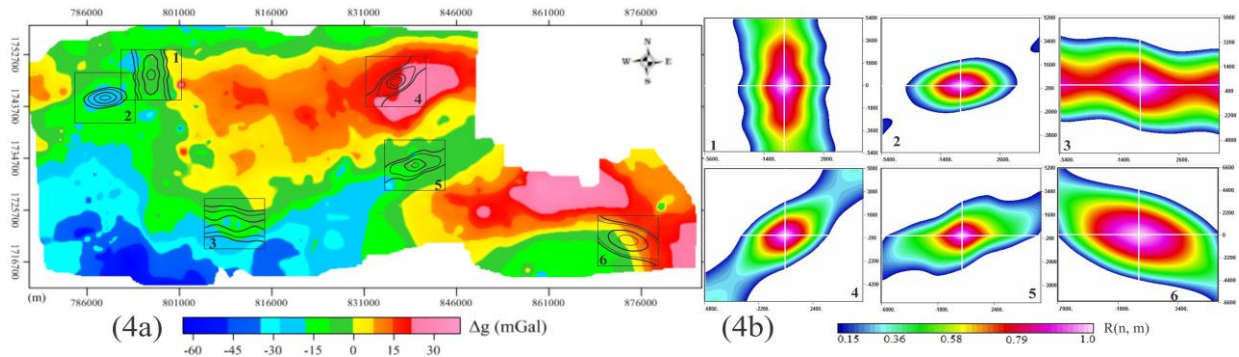


Figure 4. (4a) - The position and size of the filter window, and (4b) - The shape of the filter window corresponding to the window positions in figure (4a) determined by the two-dimensional autocorrelation function of the Nong Son - Da Nang, with the correlation radius value $R(m, n) \geq 0.15$.

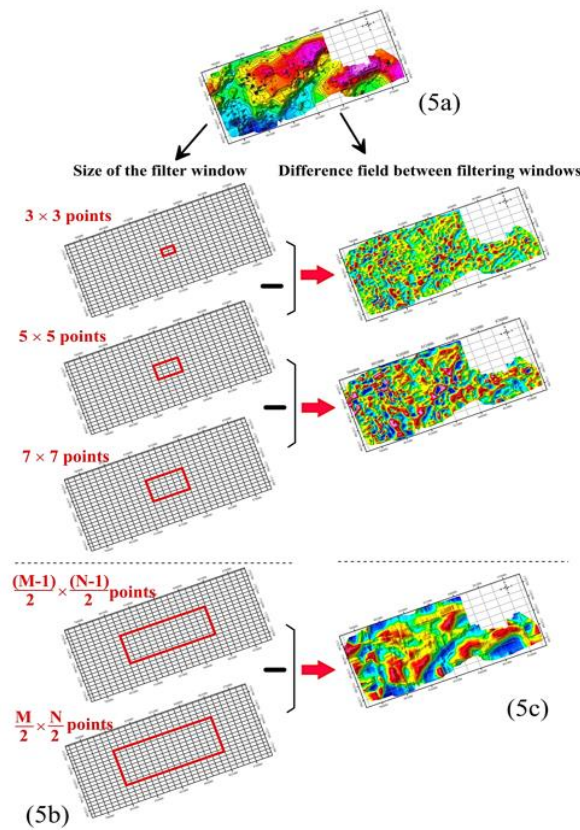


Figure 5. (5a) - Bouguer gravity anomaly; (5b) - The filter window size is increased gradually; (5c) - Residual gravity anomaly is determined by the difference of the gravity anomaly of two successive variable-size filters of the Nong Son - Da Nang.

$$\Delta\sigma(\omega_1, \omega_2, Z) = \Delta g(\omega_1, \omega_2, 0) \cdot K \cdot \frac{S(\omega_1, \omega_2, Z)}{\int_{Z=0}^{\infty} S(\omega_1, \omega_2, Z) \cdot e^{-KS} dZ} \quad (2)$$

Where: ω_1, ω_2 are the number of waves along the Ox and Oy axis; $K = \sqrt{\omega_1^2 + \omega_2^2}$ is the radial frequency; $\Delta g(\omega_1, \omega_2, 0)$ is the gravity anomaly at the observation surface; $S(\omega_1, \omega_2, Z)$ is frequency spectrum depends on the depth; $\Delta\sigma(\omega_1, \omega_2, Z)$ is the residual density value at depth Z.

3. Calculation results and discussion

The 3D gravity inversion process according to formula (2) is continuously calculated according to the window sizes of 3x3 points (600x600 m), 5x5 points (1000x1000 m), 43x43 points (8600x8600 m) and get the result of distribution of residual density in three-dimensional space from the surface to the depth Z=7250 m.

3.1. Residual density distribution by area

In order to clearly see the distribution of the residual density of the rock in the areas of the ore points, we calculate the the residual gravity anomaly - between the gravity anomalies of the successive filter window sizes. Figure 6 shows the residual gravity anomaly between the anomalies of filters with window sizes: 7x7 points (1400x1400 m) and 9x9 points (1800x1800 m), corresponding to depth Z=750 m (Figure 6a); 13x13 points (2600x2600 m) and 15x15 points, (3000x3000 m) corresponding to depth Z=1500 m (Figure 6b); 25x25 points (5000x5000 m) and 27x27 points (5400x5400 m), corresponding to depth Z=3015 m (Figure 6c); 41x41 points (8200x8200 m) and 43x43 (8600x8600 m) points, corresponding to depth Z= 5025 m (Figure 6d).

The residual gravity anomaly in Figure 6 are inverted to get the residual density distribution at depth Z=750 m (Figure 7a), at depth Z=1500 m (Figure 7b), at depth Z=3015 m (Figure 7c); and at depth Z=5025 m (Figure 7d).

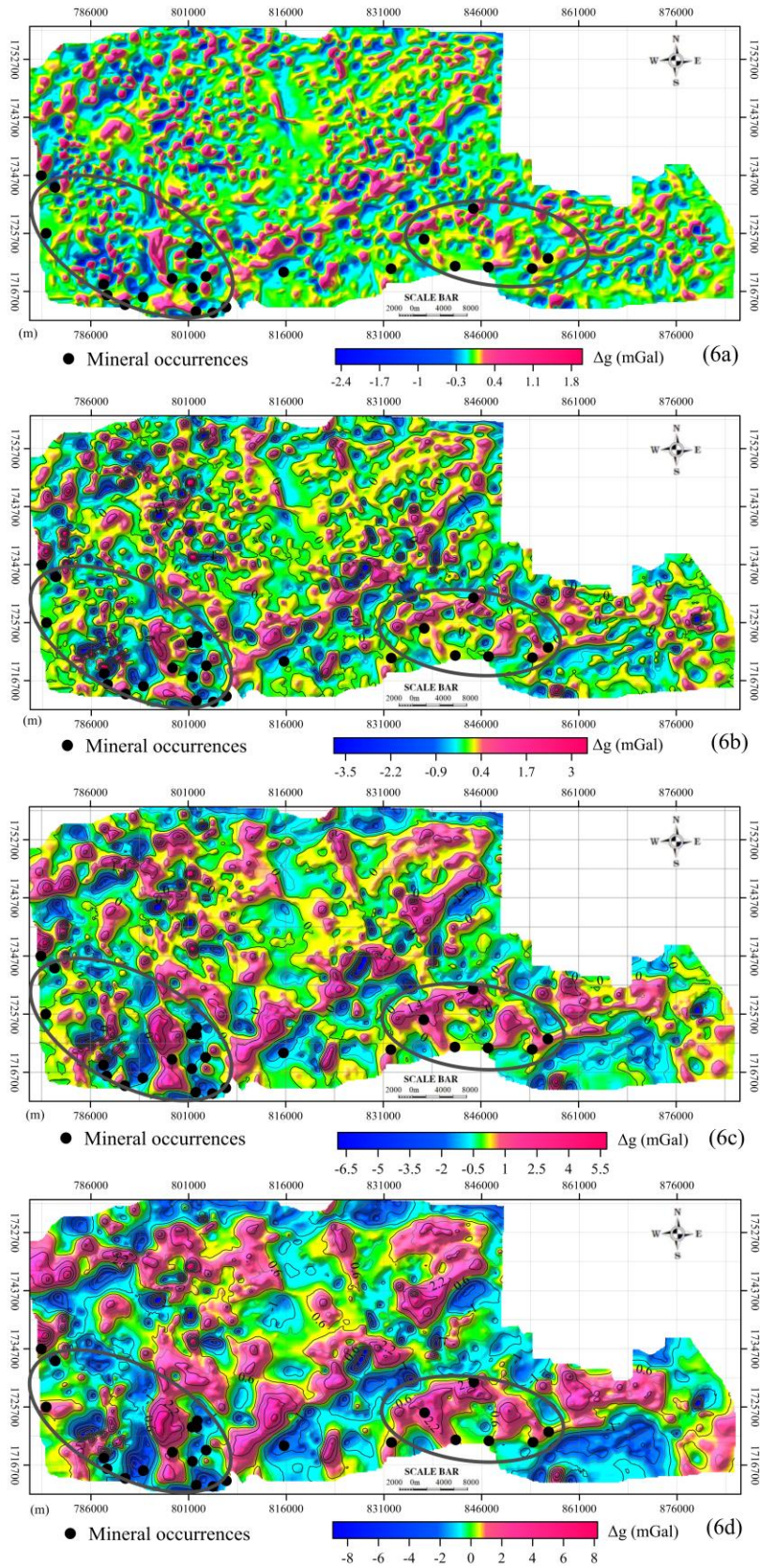


Figure 6. The residual gravity anomaly of the Nong Son - Da Nang at depth $Z=750$ m (Figure 6a); $Z=1500$ m (Figure 6b); $Z=3015$ m (Figure 6c); $Z=5025$ m (Figure 6d).

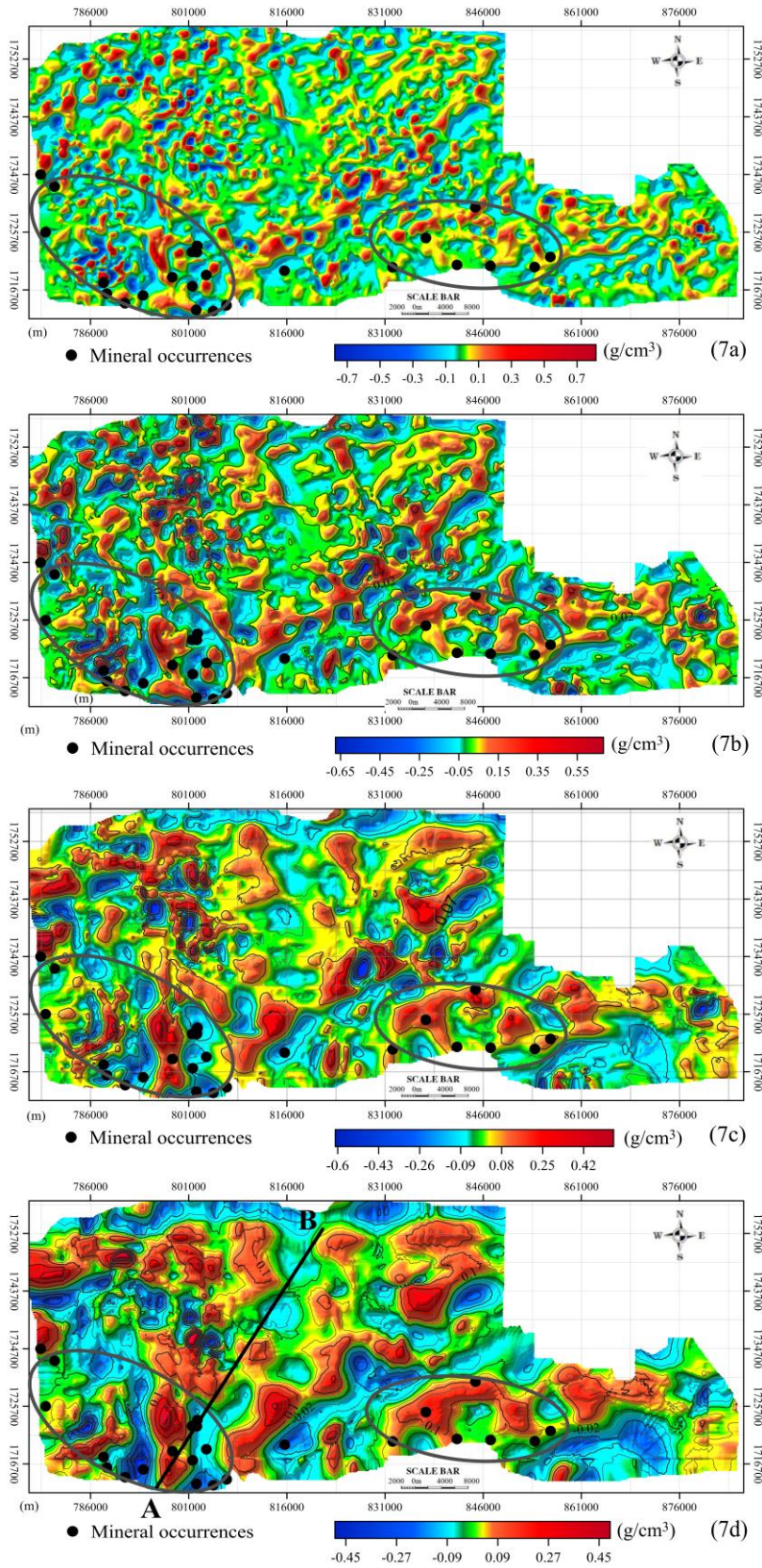


Figure 7. The residual density value distribution of the Nong Son - Da Nang at depths: $Z=750$ m (Figure 7a); $Z=1500$ m (Figure 7b); $Z=3015$ m (Figure 7c); $Z=5025$ m (Figure 7d).

At depth $Z=750$ m, the residual density value ranges from $-0.75 \div 0.7$ g/cm^3 (Figure 7a) corresponds to the residual anomaly field value ranges from $-2.5 \div 2$ mGal (Figure 6a). At depth $Z=1500$ m, the residual density value ranges from $-0.7 \div 0.6$ g/cm^3 (Figure 7b) corresponds to the residual anomaly field value ranges from $-4 \div 3.5$ mGal (Figure 6b). At depth $Z=3015$ m, the residual density value ranges from $-0.6 \div 0.5$ g/cm^3 (Figure 7c) corresponds to the residual anomaly field value ranges from $-7 \div 6$ mGal (Figure 6c). At depth $Z=5025$ m, the residual density value ranges from $-0.5 \div 0.45$ g/cm^3 (Figure 7d) corresponds to the residual anomaly field value ranges from $-9 \div 8$

mGal (Figure 6d).

3.2. Result of the distribution of the density by depth

To clarify the origin of the formation of the ore points in the study area, we examined the variation of the residual density value by depth on the survey profile A-B, where profile A-B passes through the location of ore points shown on Figure 1 and Figure 7d.

Looking at the results of Petrov's 3D gravity inversion of the residual density along profile A-B (Figure 8b), shows that at the location of the ore

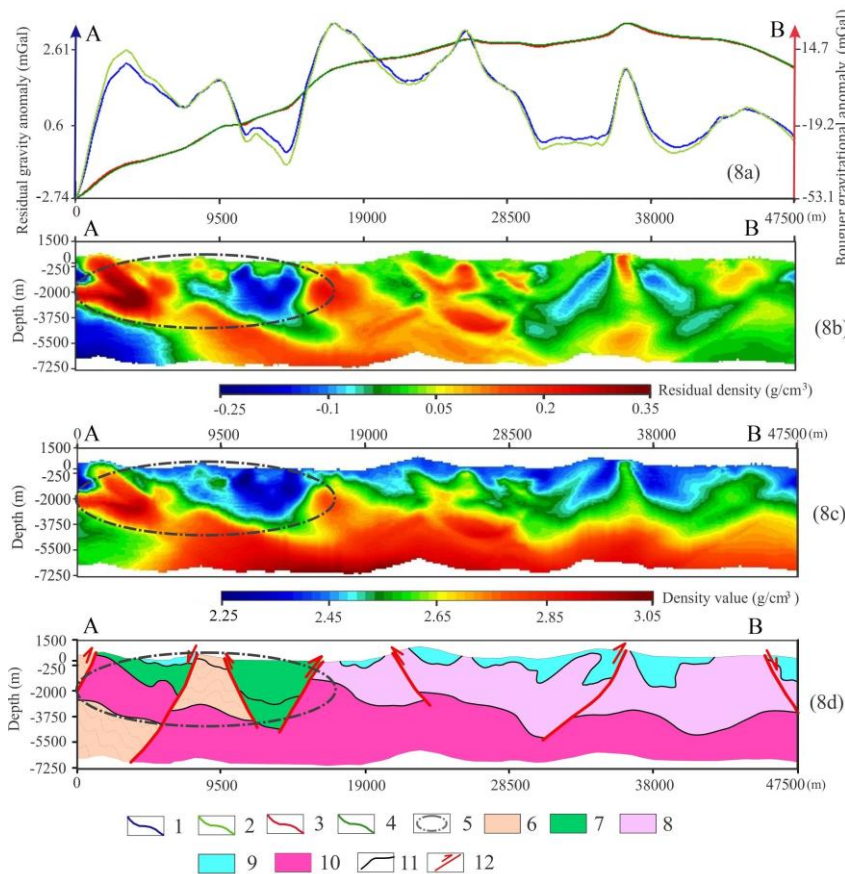


Figure 8. (8a)- The observed value of gravity anomaly and the recalculated value of gravity anomaly according to the result of 3D inversion; (8b)- Residual density value distribution along profile A-B according to the result of Petrov's 3D gravity inversion; (8c)- The true density value distribution along profile A-B according to the result of Petrov's 3D gravity inversion; (8d)- The geophysical-geological cross-section of survey profile A-B is shown in Figure 1, Figure 7d.

1- Observed residual gravity anomaly; 2- Inversion residual gravity anomaly; 3- Observed Bouguer gravity anomaly; 4- Inversion Bouguer gravity anomaly; 5- Mineral potential area; 6- Proterozoic metamorphosed sedimentary rocks; 7- Cambrian - Ordovician sedimentary rocks; 8- Triassic sedimentary rocks; 9- Jurassic sedimentary rocks; 10- Paleozoic intrusive rocks; 11- Geological boundaries; 12- Faults and displacement directions.

points the gravity anomaly is higher than the surrounding values, and the results of the inversion of the gravity anomaly obtain positive residual density value varying from $0.1 \div 0.35 \text{ g/cm}^3$, they are individually displaced in blocks to the depth $Z = 4000 \text{ m}$.

To clarify the formation mechanism of the ore point area, we convert the residual density value into the true density value of the rock with the value of density change by depth according to the law of linear transformation (Andreev, 1962) of the mass from the surface to the bottom with the chosen parameter of true density value $\sigma_{\text{surface}} = 2.25 \text{ g/cm}^3$ (corresponding to sedimentary rock) and $\sigma_{\text{bottom}} = 3.05 \text{ g/cm}^3$ (corresponding to basalt rock) (Nguyen, 2000a; Nguyen, 2014; Nguyen, 2000b) and obtained the results of real density value distribution of the rock along the profile A-B (Figure 8c). Figure 8(c) shown that at the ore point area, it is formed mainly by the magma source moving from the depths and accumulating near the surface, which is represented by the real density value bands that vary from $2.80 \div 3.05 \text{ g/cm}^3$ corresponds to the depth $Z=7250 \text{ m}$.

From the results of the 3D Petrov inversion, the rock density distribution along profile AB down to a depth of $Z = 7250 \text{ m}$ (Figure 8c), in conjunction with geological structural map (Figure 1), a geological-geophysical cross-section was subsequently interpreted (Figure 8d). The dip direction of the fault systems was inferred from abrupt lateral variations in density (Figure 8c), in conjunction with surface fault outcrops shown on the geological map (Figure 1). The boundaries of rock units were delineated based on density contrasts (Figure 8c), integrated with the regional geological map (Figure 1) and sampling data (Nguyen, 2000a; Nguyen, 2014; Nguyen, 2000b). The results indicate that: Jurassic sedimentary rocks exhibit densities ranging from $2.40 \div 2.50 \text{ g/cm}^3$; Proterozoic metamorphosed sedimentary rocks show densities of $2.50 \div 2.60 \text{ g/cm}^3$; Cambrian-Ordovician sedimentary rocks have densities of $2.25 \div 2.40 \text{ g/cm}^3$; Triassic sedimentary rocks display densities of $2.60 \div 2.70 \text{ g/cm}^3$; Paleozoic intrusive rocks are characterized by densities of $2.70 \div 3.05 \text{ g/cm}^3$.

The interpretation results (Figure 8d) indicate that fault systems within the

displacement zone have induced brittle, ductile, plastic, and re-metamorphic deformation in the surrounding rocks, resulting in variations in density and other geophysical properties. These deformation processes create favorable conditions for the ascent of hydrothermal fluids, which may lead to the development of potential mineralized zones associated with the upward migration and near surface accumulation of magma derived materials.

4. Conclusions

The major conclusions of this study are the following:

- Petrov's 3D inversion is effective in processing the Bouguer gravity anomaly to determine the residual density value distribution of the anomalous object by area and depth.

- At the sites ore points of the southwest, the residual density value of the rock varies from 0.1 g/cm^3 to 0.35 g/cm^3 , corresponds to the residual anomaly field value ranges from 1 mGal to 3.5 mGal , and extends to a depth of $Z = 4000 \text{ m}$.

- The true density value varies from surface to depth $Z = 7250 \text{ m}$ from $2.25 \div 3.05 \text{ g/cm}^3$, at the locations of ore points in the southwest, the density value varies from 2.8 g/cm^3 (on the ground surface) to 3.05 g/cm^3 (at a depth of 7250 m).

- The results of Petrov's 3D inversion of the Bouguer gravity anomaly in the Nong Son - Da Nang provide initial information on residual density value of rocks at sites of ore deposits and in the whole studied area, so that geophysicists and geologists can have an overview and make accurate decisions in the next detailed research phases.

Acknowledgements

The authors would like to thank the research project of the Hanoi University of Mining and Geology (code T25-08). We also deeply thankful to Prof. Dr. Sci. Vladimirovich Aleksey Petrov for providing support with the "COSCAD 3D" software. In addition, we would like to thank my colleagues and the anonymous reviewers for their valuable time and constructive comments on this paper.

Contribution of authors

Hong Thi Phan - methodology; collection, synchronization, and processing of gravity data; writing and editing of the final manuscript; Phuong Minh Do - synthesis of geological documents; interpretation of processing results; Vladimirovich Aleksey Petrov - processing of gravity data.

References

Andreev B. A., Klushin I. G. (1962). *Geological interpretation of gravity anomalies*. Leningrad, Gostoptekhizdat, 496 pages (in Russian).

Blakely, R. J. (1996). *Potential theory in gravity and magnetic applications*. Cambridge University Press. 197 pages. <https://www.cambridge.org/core/books/potential-theory-in-gravity-and-magnetic-applications/348880F23008E16E663D6AD14A41D8DE>.

Hai T. T., Khin Zaw, Jacqueline A. H., Takayuki M., Sebastien M., Chun-Kit L., Youjin L., Hai V. L., Sang D. N. (2014). The Tam Ky-Phuoc Son Shear Zone in central Vietnam: Tectonic and metallogenic implications. *Gondwana Research* 26, 144-164. https://www.researchgate.net/publication/249644706_The_Tam_Ky-Phuoc_Son_Shear_Zone_in_Central_Vietnam_Tectonic_and_metallogenic_implications.

<http://www.coscad3d.ru/index.php>.

Nikitin A. A., Petrov A. V. (2008). Theoretical foundations of geophysical information processing. *Science and Technology Publishing House*. Moscow, Russia, 127 pages. (in Russian) <https://www.geokniga.org/bookfiles/geokniga-nikitinteorosnovygeofizinfo2008.pdf>.

Nikitin A. A. (1986). *Theoretical bases of geophysical information processing*. Moscow 342 pages. <https://www.geokniga.org/books/4894?ysclid=mgubo16q72809204897>.

Nguyen T. L. (2000a). Aeroradiometric Survey at 1:50,000 Scale and Gravity Survey at 1:100,000 Scale in the Central Region of Vietnam. *Geological Information and Archives Center*, Hanoi, 147 pages (in Vietnamese).

Nguyen T. L. (2014). Aeroradiometric Survey at 1:50,000 Scale and Gravity Mapping at 1:100,000 Scale in the Southern Pleiku Area. *Geological Information and Archives Center*, Hanoi, 177 page (in Vietnamese).

Nguyen X. S. (2000b). Flight results measured from 1: 50,000 scale gamma spectrum and measured in Kon Tum area. Center for Information, *Geological Archives*, Hanoi, 174 pages. (in Vietnamese).

Nguyen X. B., & Tran D. L. (1983). Geological map of Vietnam, scale of 1:500,000. *Archived at the Center for Geological Information and Archives*, Hanoi, Vietnam. (in Vietnamese).

Nguyen X. B. (1995). Report on the revision of the geological and mineral map of Southern Vietnam, scale of 1:200,000. *Archived at the Center for Geological Information and Archives*, Hanoi, Vietnam. (in Vietnamese).

Petrov A. V., Yudin D. B., Soeli Hou (2010). Processing and interpretation of geophysical data by methods of a probabilistic-statistical approach using computer technology "COSCAD 3D". *Earth sciences, №2*, UDC 551-214, 126-132. (in Russian) http://www.kscnet.ru/kraesc/2010/2010_16/art13.pdf.

Phan T. H., Petrov A. V., Do M. P. (2020). Processing and interpretation of gravity data anomalies in the central Vietnam using the «COSCAD 3D» computer technology. *Young-earth sciences, MGRI-RGGRU, Moscow, 293-297*. [https://www.mgri.ru/science/scientific-practical-conference/2020/TOM%204%20\(1\).Pdf](https://www.mgri.ru/science/scientific-practical-conference/2020/TOM%204%20(1).Pdf).

Phan T. H., Petrov A. V., Do M. P. (2021). Zoning of prospects for hidden magma blocks in the central Vietnam based on the analysis of magnetic anomaly data. *II Youth scientific and educational conference, SINGRI, Moscow, №4*, 123-127. https://www.tsnigri.ru/images/conf/Tezis_X_Conf_2021.pdf.

Phan T. H., Petrov A. V., Do M. P. (2021). Application of a two-dimensional filtering algorithm in a sliding window of a "live" form on the example of central Vietnam. *New ideas in earth sciences, MGRI-RGGRU, № 4*, 339-343. <https://mgri.ru/science/scientific-practical->

- conference/2021/%D0%A2%D0%BE%D0%BC%204.pdf.
- Phan H. T. (2022). Computer technology for interpretative processing of gravity and magnetic exploration data using probabilistic-statistical approach methods (using the territory of central Vietnam as an example). *Doctoral thesis*, 120 pages. <https://www.dissercat.com/content/kompyuternaya-tehnologiya-interpretatsionnoi-obrabotki-dannykh-gravirazvedki-i-magnitorazve?ysclid=mh1raw9cs7741021513>.
- Petrov A.V. (1997), Methods of adaptive filtering and multivariate analysis of variance in the computer system for processing geophysical information "COSCAD 3D". *Doctoral thesis*, 192 pages. https://rusneb.ru/catalog/000199_000009_000046168/?ysclid=mgugr4iydk865182265.
- Yudin D. B. (2011). Computer technology for processing geophysical information organized into profile observation networks using probabilistic-statistical methods. *Doctoral thesis technical sciences*. 150 pages. <https://www.dissercat.com/content/kompyuternaya-tehnologiya-obrabotki-geofizicheskoi-informatsii-organizovannoi-v-profilnye-s?ysclid=mh1r96cvr4292427282>.